Deep-Sea Research I 102 (2015) 78–89

Contents lists available at ScienceDirect

Deep-Sea Research I

journal homepage: www.elsevier.com/locate/dsri

Depths, migration rates and environmental associations of acoustic scattering layers in the Gulf of California

David E. Cade [a,1], Kelly J. Benoit-Bird [a,*]

[a] College of Earth, Ocean, and Atmospheric Sciences (CEOAS), Oregon State University, 104 CEOAS Administration Bldg, Corvallis, OR 97331, USA

ARTICLE INFO

Article history:
Received 11 December 2014
Received in revised form
29 April 2015
Accepted 4 May 2015
Available online 14 May 2015

Keywords:
Gulf of California
Acoustic scattering layers
Diel vertical migration
Oxygen minimum zone
Logistic modelling

ABSTRACT

The ecology in the Gulf of California has undergone dramatic changes over the past century, including the emergence of Humboldt squid (*Dosidicus gigas*) as a dominant predator. In the face of these changes, we compare the ubiquitous and ecologically important concentrations of mid-water organisms that comprise acoustic scattering layers to published results, describing their occurrence in detail and showing that they remain similar to features described 50 years previously. To classify scattering layers in the region, we applied an automatic detection algorithm to shipboard echosounder data from four cruises. We consistently detected a broad (>200 m) background layer with a mean daytime bottom boundary depth of 463 ± 56 m (night: 434 ± 66 m), a near-surface layer with mean daytime bottom depth of 43 ± 40 m (night: 61 ± 38 m), and a main migrating layer with mean bottom depth of 333 ± 76 m (night: 54 ± 27 m). Diel vertical migration rates for dusk ascents reached a maximum, on average, of 8.6 ± 3.1 cm s^{-1}, and dawn descents averaged a maximum of 6.9 ± 2.4 cm s^{-1}. Deep scattering layers were often found concurrent with regions of severe hypoxia and we used environmental data to test for the association of scattering layer boundaries with environmental parameter values. Although results were inconsistent, we found scattering layer depths to be more highly associated with temperature and density than with oxygen. These results suggest that the recent success of *D. gigas* in the Gulf of California is not likely to be attributable to the effects of shoaling oxygen minimum zones on acoustic scattering layers.

1. Introduction

In every ocean horizontally-extensive, continuous mid-water features known as acoustic scattering layers have been identified using echosounders (Tont, 1976; O'Brien, 1987). Composed of densely concentrated planktonic and nektonic organisms whose echoes cannot be individually resolved (Barham, 1966; Tont, 1976), scattering layers are found throughout the entire water column from surface layers down to at least 2000 m (Burd et al., 1992; Opdal et al., 2008). Most commonly, the organisms detecting in scattering layers are krill, shrimp, small squid, and mesopelagic fish species like myctophids (Butler and Pearcy, 1972; Simard and Mackas, 1989; Benoit-Bird and Au, 2002). A single layer can be on the order of meters to tens of meters thick (Sameoto, 1976; Thomson et al., 1992), and can be hundreds of kilometers in extent (Chapman and Marshall, 1966). It is no surprise, therefore, that the mesopelagic organisms detected in these features are keystone components of pelagic ecosystems (McGehee et al., 1998; Fock et al., 2002; Hays, 2003) and contain an estimated 10 billion tons of mesopelagic fish worldwide, likely representing the bulk of fish biomass in the oceans (Irigoien et al., 2014).

In the Gulf of California, the primary study on scattering layer characteristics was completed nearly fifty years ago (Dunlap, 1968). This region, however, has gone through extensive ecological changes in that time period and there have been substantial changes in the degree of human influence in the region both locally, where the population and associated pressures of just the peninsula side increased nearly 30-fold between 1940 and 2010 (Instituto Nacional de Estadística y Geografía, 2014), and regionally due to climate change, increased agricultural runoff and the diversion of nearly all of the freshwater input from the Colorado River (Rodriguez et al., 2001). As a result, the biota in the region has undergone striking changes. In a recent study, Sagarin et al. (2008) found dramatic losses of intertidal species abundance and diversity and substantial decreases in pelagic species abundance in the region relative to descriptions provided by Steinbeck and Ricketts (1941).

Abbreviations: CI, confidence interval; CTD, conductivity, temperature and depth sensor; DSL, deep scattering layer; DVM, diel vertical migration; OMZ, oxygen minimum zone; PAR, photosynthetically active radiation; SOR, standardized odds ratio

* Corresponding author. Tel.: +1 541 737 2063.
E-mail addresses: davecade@stanford.edu (D.E. Cade), kbenoit@coas.oregonstate.edu (K.J. Benoit-Bird).
[1] Present address: Department of Biology, Hopkins Marine Station, 120 Ocean View Blvd, Stanford University, Pacific Grove, CA 93950, USA.

http://dx.doi.org/10.1016/j.dsr.2015.05.001
0967-0637/

A significant change in the biota noted by Sagarin et al. (2008) is the appearance, likely in the 1970s, of one of the region's most important predators, the Humboldt squid (*Dosidicus gigas)* (Rosas-Luis et al., 2008). Humboldt squid are voracious predators whose diet is dominated by scattering layer organisms, primarily the myctophids *Benthosema panamense* and *Triphoturus mexicanus* and the small squid, *Pterygioteuthis giardi* (Markaida et al., 2008). Indeed, studies of squid diet and behavior have been a primary source of insight into the composition and distribution of mid-water fishes in the Gulf (Markaida et al., 2008). Since *Dosidicus* is well-adapted to low-O_2 environments (Rosa and Seibel, 2010), and because their abundance in other regions has been correlated with prey abundance (Stewart et al., 2014), it has been proposed that squid are successful in the Gulf because of the proximity of deep scattering layers to a shallow, extensive oxygen minimum zone (OMZ) (Robison, 1972; Markaida et al., 2008).

The OMZ in the Gulf of California is extensive, with hypoxic waters (< 0.5 mL $L^{-1} \approx 1.7$ kPa) extending from 200 m to 1200 m depth on average, and is overlain with a narrow oxygen limited zone (0.5 mL $L^{-1} \approx 1.7$ kPa $< O_2 < 1.5$ mL $L^{-1} \approx 5.1$ kPa) that overlaps with the euphotic zone (Gilly et al., 2013). What is not known is to what degree the depth of the OMZ controls the depth of scattering layers. If the features are linked, as suggested by Gilly et al. (2013), then *Dosidicus* may have greater success when OMZs shoal because their food sources are squeezed into a smaller portion of the water column. If the two features are not linked, however, then a shallow OMZ may influence the success of *Dosidicus* by bringing an environmental habitat to which they are well-adapted within range of prime feeding grounds, and their prey would be increasingly exposed to low-oxygen water in which they typically reduce their activity (Childress and Seibel, 1998). It has been shown that El Niño Southern Oscillation (ENSO) events strongly influence squid distribution in the Gulf (Rosas-Luis et al., 2008; Hoving et al., 2013) and the relationship of environmental conditions to scattering layer distribution may help explain some of this habitat shift. The questions of what factor or factors control scattering layer depth, and how scattering layer characteristics have changed from fifty years ago are thus of importance to the ecology and management of this important fishery species.

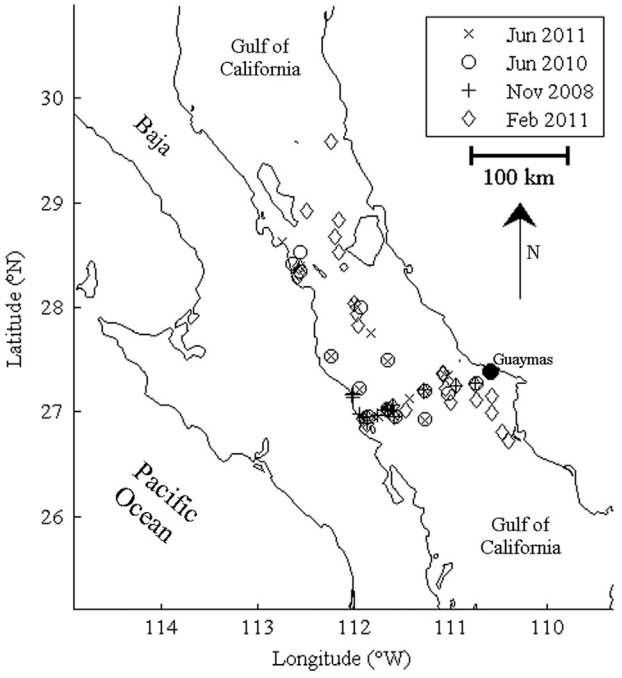

Fig. 1. Map of the research area in the Guaymas Basin in the Gulf of California (CEC, 2009). Symbols indicate CTD profile collection locations for all four cruises.

In other regions, along with oxygen (Devol, 1981; Bertrand et al., 2010) additional environmental factors have been linked with the depths of scattering layers including light (Clarke, 1970), density layering (Herdman, 1953; Weston, 1958), thermocline depths (Kumar et al., 2005), low-salinity water (Forward, 1976), and pressure (Forward and Wellins, 1989). Under various conditions, each of these environmental variables has been shown to play a role in controlling organisms' depth after a nightly surface feeding foray. This process, known as diel vertical migration (DVM), is commonly observed in scattering layers and has important implications for turbulent mixing, biogeochemical cycling, the transport of nutrients and gases, and the life cycles and behavior of scattering layer organisms and their predators (Longhurst et al., 1990; Steinberg et al., 2000; Kunze et al., 2006; Bianchi et al., 2013).

The gaps in our understanding of scattering layer behavior in the Gulf of California, the broad ecological implications of changes in this behavior, and the potential links between environmental conditions and scattering layers have inspired our study's two goals: (1) to describe general features of acoustic scattering layers in the Gulf of California, including rates of DVM, and (2) to understand the environmental forces in the region that determine the depths of these layers. As Childress and Seibel (1998) point out, "within a given geographic area, [environmental parameters] are almost hopelessly confounded and it is difficult, if not impossible, to demonstrate an adaptive response to one" of the variables. Using acoustic data from four research cruises, we described layer features and attempt a comprehensive analysis that would untangle the influence of environmental variables on the vertical positions of these mixed assemblages.

2. Methods

2.1. Summary of approach

Data for this study were collected on four multi-week cruises in the Guaymas Basin region of the Gulf of California (Fig. 1) in November 2008, June of 2010, February of 2011, and June of 2011. Conductivity, temperature, depth (CTD), oxygen and light profiles were collected a total of 103 times, and acoustic data were recorded continuously. Scattering layers within acoustic echograms were identified by applying an automatic layer detection algorithm to all data, enabling each layer's depth and migration speed to be tracked. The scattering layers surrounding the CTD profile sites were subsequently examined and three statistical approaches were used to study the environmental context in which the layers appear.

2.2. Field site and data collection

The Gulf of California is a 1000 km long, 160 km wide subtropical body of water characterized as a series of troughs, ridges and basins that range in depth from 100 to 3600 m (Rusnak et al., 1964). The water masses making up the Gulf are strongly affected by Pacific Ocean fluctuations including El Niño, with surface temperatures ranging from 16 °C in winter to 31 °C in summer and a surface salinity typically above 35 (Robles and Marinone, 1987) that decreases with depth.

Acoustic data from the two June cruises aboard the RV New Horizon were collected with Simrad EK60 split-beam, pole-mounted echosounders at 38, 70, 120 and 200 kHz with 512 μs pulse lengths. The 38 kHz transducer had a 12° beam-width and the others had 7° beam widths. For the November and February cruises, acoustic data collection was from the RV BIP XII with a

38 kHz single-beam (15°) and a 120 kHz split-beam (7°), hull-mounted transducer. The November cruise used 1024 and 256 μs pulse lengths for the 38 and 120 kHz transducers, respectively, while the February cruise used 512 μs pulse lengths (Benoit-Bird and Gilly, 2012).

Profiles of environmental characteristics were collected with CTD sensors equipped with a dissolved oxygen sensor, a fluorometer and, for the June cruises, a photosynthetically active radiation (PAR) sensor. Fluorescence dropped below detectable levels much shallower than most scattering layers, so no associations were found and this parameter was excluded from most displayed results. All environmental data were averaged into 1 m depth bins. Of the 103 profiles, 49 were collected in deep water basins >600 m and 54 were collected in shallower water within 20 nmi of the coast. To ensure accurate acoustic results, only the top 600 m of the water column were examined; in all cases this was sufficient to encompass the entire background scattering layer. For consistency, only the 55 profiles taken during the daylight hours that included regions of severe hypoxia (<22 μmol $kg^{-1} \approx 0.5$ mL $L^{-1} \approx 2.2$ kPa as per Hofmann et al., 2011) above 600 m were used in most analyses of the deep scattering layers that occur below the thermocline. Twenty CTD profiles were collected during the June 2011 cruise (16 of which met the criteria for inclusion), 14 (9 which met the criteria) were collected in June 2010, 27 (11) were taken in November 2008 and 42 (19) in February 2011.

Temperature, density, salinity, dissolved oxygen, light level and fluorescence profiles were collected, and the gradient of each parameter was also calculated from the environmental data that had been averaged into 1 m depth bins and then included in analysis. We determined the base of the thermocline at each site as the deepest consecutive depth at which the temperature gradient was larger (in an absolute sense) than one standard deviation above the mean of the logged temperature gradients. For oxygen, we chose to record and test results in partial pressure units (kPa) as evidence is accumulating that this is the biologically relevant measure of oxygen (Hofmann et al., 2011), although other metrics of dissolved oxygen concentration were also tested for comparison. For light, we used PAR values, a direct measure of the total light received at a given depth (measured in μE m^{-2} s^{-1}, equivalent to μmol photons m^{-2} s^{-1}). Despite the possibility that scattering layer organisms cue off of other aspects of irradiance, PAR tends to decrease in synchrony with other measures of light more applicable to zooplankton (Cohen and Forward, 2005) and is easily and routinely measured. Although we collected light data during both June New Horizon cruises, in the 2010 cruise the PAR readings dropped below detectable levels within 34 m of the surface for all casts. Therefore, in the analyses below, light was only included as a parameter for the June 2011 cruise.

2.3. Scattering layer identification and analysis

Scattering layers were identified and classified into background layers and internal strata using an automatic detection algorithm (Cade and Benoit-Bird, 2014). Background layers were defined as contiguous regions of acoustic energy above a threshold, and internal strata were defined as continuous features of high acoustic energy within a background layer whose echo amplitudes approached a Gaussian distribution. Migrating layers were most commonly classified as strata, although at times a shallow (<100 m deep) stratum encompassed the entire thickness of a background layer. The algorithm worked by identifying potential layer/stratum boundaries in each vertical column of acoustic data, and then linking those boundary points horizontally according to user-defined parameters. The most important parameters affecting layer detection were threshold (which we set at -78 dB) and maximum vertical linking distance (set at 40 m). Other parameters used for layer detection had smaller effects, but are listed in the Gulf of California analysis in Cade and Benoit-Bird (2014).

To analyze general scattering layer properties, the layer detection algorithm was applied to all data in 24-h increments (Fig. 2). Data from the 38 kHz transducer were used primarily for this analysis since that frequency provided the largest depth range and was closer to the frequency used in earlier analyses (Dunlap, 1968).

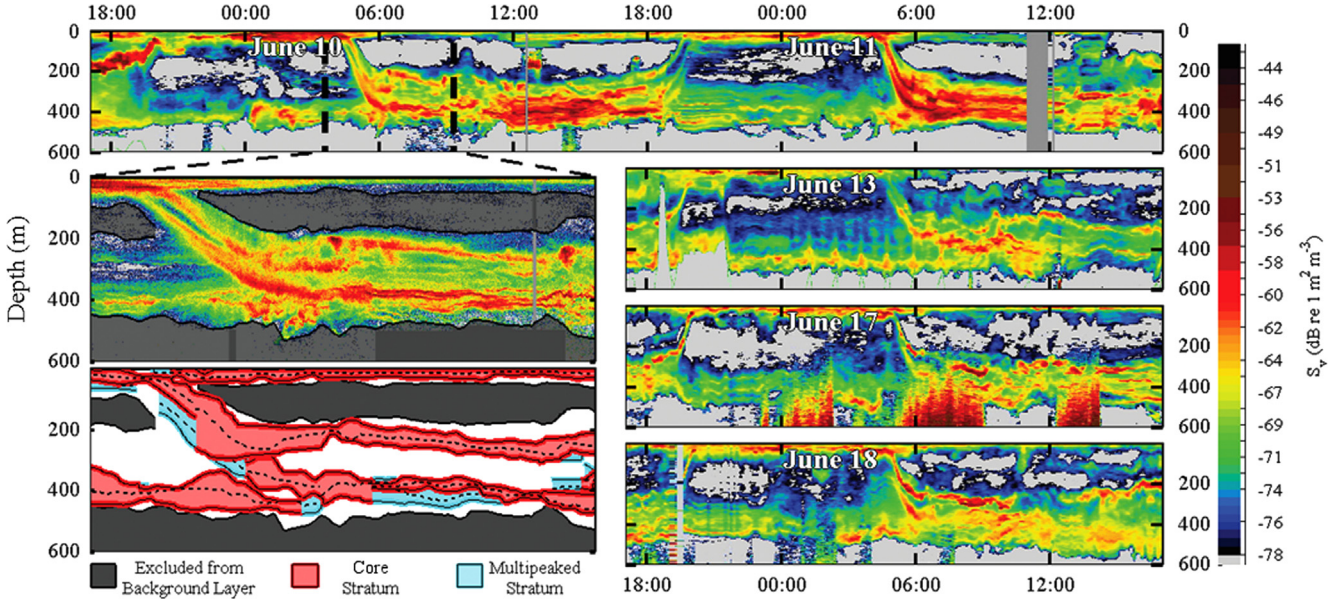

Fig. 2. Scattering from a 70 kHz transducer mounted on a moving vessel over several days in deep water. The continuity of the main migrating stratum is readily apparent and is contiguous for hundreds of kilometers. Similar diel vertical migration patterns can be observed over several days and several regions. The insets highlight the different kinds of scattering layers referenced in this analysis. Contiguous regions of energy above an acoustic threshold are referred to as background layers. The top inset outlines the background layer and grays out regions of the water column that are not part of the layer. The bottom inset highlights internal strata from the data above, highlighting in red the dense energy regions described as core strata, and highlighting in blue the multipeaked strata where smaller peaks in the energy spectrum overlap vertically with the core strata. The dashed lines track the peak energy within the strata. See Cade and Benoit-Bird (2014) for a full description of layer classifications and the layer detection algorithm. Times shown are local time.

The depths of the bottoms of the background layer, the shallowest (upper) stratum and the main migrating stratum were recorded every 5 km and the mean depth was calculated. Although all cruises were of similar time lengths, there were more data points in the June 2011 cruise due to cruise characteristics more conducive to better acoustic data collection including slower cruising speeds and overnight transects. When calculating the average daytime and nighttime layer depths, times between sunset/sunrise and nautical twilight were left out of analysis to exclude the effect of migrating layers. To calculate the ascent and descent speeds of the migrating layers specifically, the layer bottom depth at the time when the migrators at the bottom of the layer first started to rise (or descend) was compared to the depth and time of vertical stabilization for every dusk or dawn event on each research cruise. The migrating speed of the fastest 100 m migration segment was also recorded as a way to compare migration speeds to other results that report maximum migration rates (e.g. Barham, 1966; Kaltenberg et al., 2007). For surface light levels, two minutes of data were averaged at the time of migration initiation/completion. The measurements were compared using standard t-tests.

For our analysis considering correlations of environmental parameters with layer depth, scattering layers were detected in a region surrounding the location of each CTD deployment, this region is referred to throughout the text as a "CTD region". For each profile, a three km region before the ship stopped to collect the profile was selected as representative of the region. In some circumstances, for instance if the ship's motion before the CTD profile involved a large change in bottom depth, a 3 km region from after the CTD deployment was chosen. In each section of data around a CTD collection site, an average bottom depth and top depth of each scattering layer in the region of interested was recorded, as well as the average depth of the seafloor. For the internal strata, the average depth of the peak energy in each layer was also noted. For these analyses, both 38 kHz and 70 kHz data were used as both had sufficient resolution down to 600 m.

2.4. Tests for association of scattering layers with environmental parameters

After initial tests illuminating the correlations between environmental parameters were run, we conducted three increasingly specific statistical tests in an attempt to determine which parameters had the greatest likelihood of influencing scattering layer depths in our study areas. To account for the possibility that a parameter may only influence layer depth in a subset of the data, statistical analyses were done not just on the data as a whole, but on as many subsets of the data as possible. Subsets included the transducer frequency at which the layer was detected (70 or 38 kHz), geographic region, bottom depth, hypoxia status of deep water, season, diel period, layer type, depth bin of the layer, and type of layer depth determination. Three different determinations of the "depth" of the layer were also tested in all methods: layer bottom, top, and the depth of peak energy.

The first analysis, the simplest, was performed to find the specific values of environmental parameters at each layer feature depth and to determine if specific values tended to occur at each feature. After locating the depths of the scattering layer features, the value of each parameter of interest in each data region was recorded and plotted (as in Fig. 3). A central value was calculated, and then the depth at which the environmental parameter reached that value in each data region was plotted against the depth of the scattering layer, with strong correlations indicating a likely relationship. This method was used by Bertrand et al. (2010) to assert that acoustic scatterers in their study area were restricted to a region of the water column above the depth of the 0.8 mL L^{-1} O_2 level.

The second method attempted to better separate the influence of each environmental parameter on scattering layer depths. A χ^2 contingency table analysis was used to look for non-random patterns (Wackerly et al., 2008) in the association of each scattering layer feature with each parameter. The water column was first divided into bins based on parameter concentration, and the number of layers that occurred in the water column with that concentration were tallied. A χ^2 test was performed on the number of occurrences of the feature in each bin and a p-value was calculated. Features that were more likely to occur at specific values of only one parameter could then be identified by looking for regions in which only one parameter had a significant (<0.05) p-value.

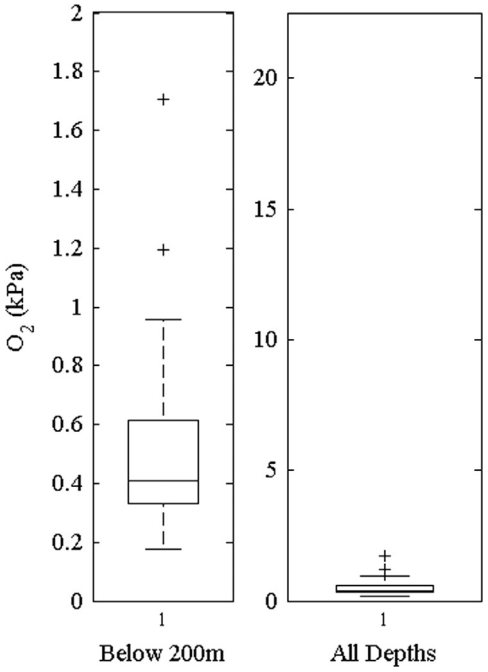

Fig. 3. The oxygen content at the bottom of the 70 kHz background layers in the 28 CTD regions from each New Horizon cruise that had a region of severe hypoxia. When plotted against the whole water column, the range (0.17–1.7 kPa) appears very small. When plotted against the values below 200 m, the association of layer bottoms with a specific oxygen level appears less strong.

The third analysis done to identify important parameters associated with scattering layer depths was an examination of the coefficients and the fit of logistic models (Ramsey and Schafer, 2013). The models shown in Fig. 4 depict the probability of a feature occurring at each depth, given the environmental profiles and depth of feature occurrence at the rest of the CTD regions. The CTD profiles for each parameter (and their gradients), depth, and the bottom depth were used as explanatory variables in the models. The dependent variable was a column of 1s and 0s indicating the presence or absence of the feature of interest at each depth. Each model was created with five different versions of the dependent variable; each version indicated whether, at each depth, there was a layer feature (top, bottom or peak energy) within 0, 5, 10 or 20 m of the depth. A fifth dependent variable indicated whether each depth was within the boundaries of a layer. A stepwise logistic regression was performed for each region of interest and the coefficients were examined. An explanatory variable was kept in the model if there was a significant ($p<0.05$) drop in deviance when it was excluded. A p-value was calculated for each parameter that was kept in the model. Models were examined for fit both manually and using a Homer–Lemeshow test. The logistic models were tested by a leave-one-out method, constructing a model for each specific CTD region without the information from that region in the model. The model-generated probability of occurrence of the feature of interest was then plotted against the actual features. Akaike and Bayesian Information Criteria (AIC and BIC, respectively) were also calculated to compare models of

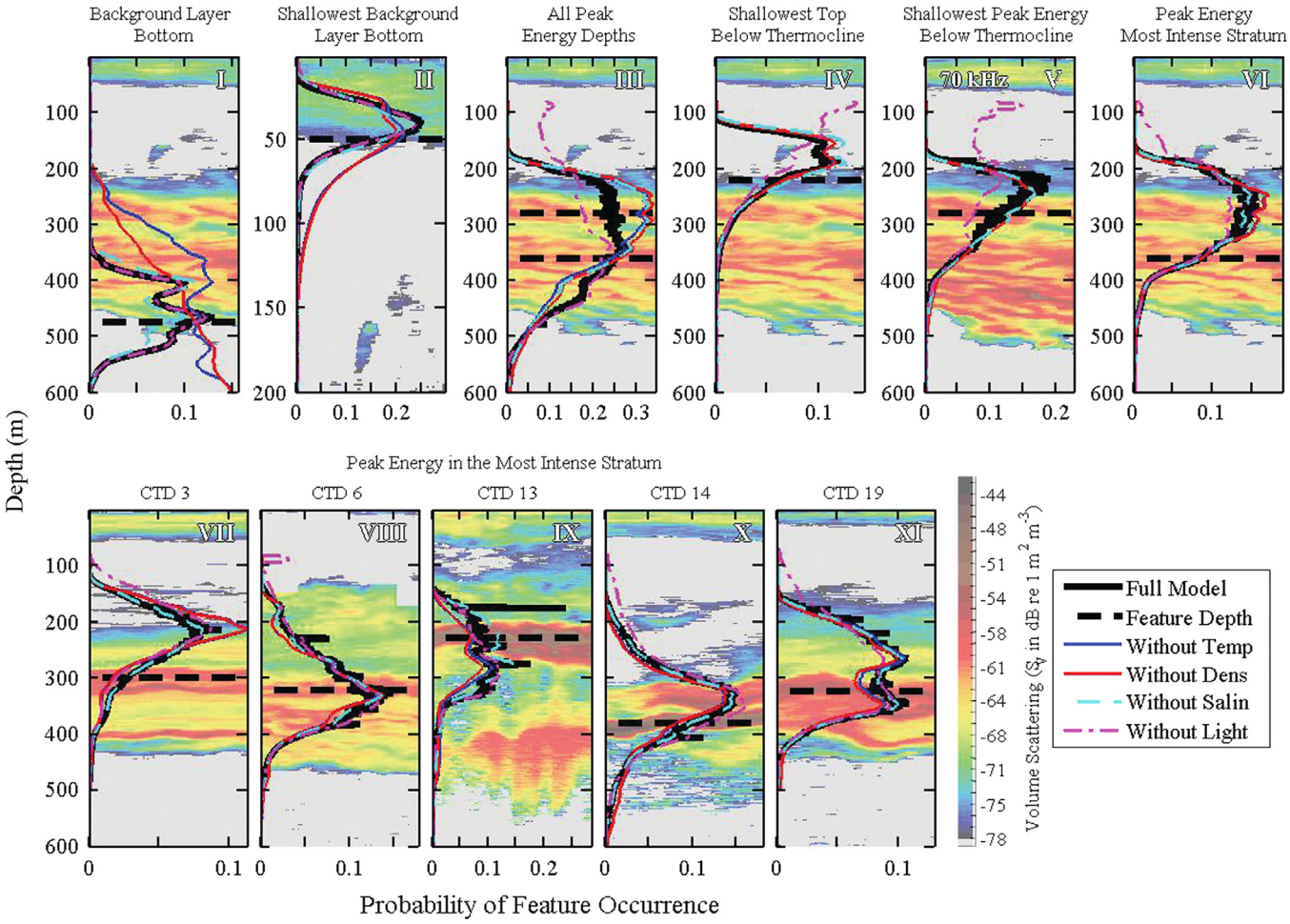

Fig. 4. Logistic model results from the June 2011 data predicting the depth of feature occurrence based on environmental parameters. Except as indicated, all depicted data are from a 38 kHz transducer. The top row shows the same region (around CTD 2) with the results from models that used different scattering layer features as the output parameter. The bottom row (and graph VI) shows the results from different regions of a model predicting the depth of the peak energy of the most acoustically dense stratum. Also depicted are models constructed after excluding oxygen, temperature, density or light from the model. Models were also constructed after excluding other parameters, but results were not substantially different than the full model.

Table 1
Depths (m) of the bottom of acoustic scattering layers in the Gulf of California collected with a 38 kHz echosounder. sd = standard deviation, n = # of observations.

	Background layer						Upper stratum						Migrating stratum					
	Day			Night			Day			Night			Day			Night		
	mean	sd	n	**mean**	sd	n	**mean**	sd	n	**mean**	sd	n	**mean**	sd	n	**mean**	sd	n
Jun 2011	**485**	40	193	**470**	40	104	**42**	40	200	**58**	30	141	**329**	86	206	**57**	19	137
Jun 2010	**445**	53	123	**408**	66	66	**46**	34	152	**58**	53	98	**356**	50	105	**46**	25	72
Nov 2008	**341**	39	16	**336**	12	20	**36**	42	11	**68**	24	88	**280**	59	33	**57**	37	76
Feb 2011	Not available						**53**	62	35	**75**	36	65	**321**	52	16	**52**	28	62

similar complexity. The significance of each parameter to the model was calculated by examining a standardized odds ratio (SOR). To calculate SOR, the coefficient of each parameter in the logistic model was multiplied by the absolute value of a measure of its variability, giving the log odds that an increase (or decrease) of this amount would have an effect on the probability of occurrence of the feature in the model. The exponential of the log odds was recorded as the SOR. An SOR close to 1 implied that there was little effect of the parameter on the probability of occurrence of the feature. A large SOR, however, implied a large influence on the feature. We rejected standard deviation as an appropriate measure of variability because the standard deviation of each parameter was affected by large changes above the thermocline that may not be applicable near the feature of interest. Instead we calculated the median change in parameter value of a depth change of 10 m at the average depth of the target feature, and used this as our measure of variability.

3. Results

3.1. Scattering layer characteristics

The depths of the 38 kHz acoustic scattering layers in the Gulf of California over the four research cruises are reported in Table 1.

Table 2
Timing of the initiation and termination of DVM, with associated surface light levels.

	Start of ascent									Start of descent								
	Time before sunset (min)			Light level ($\mu E\ m^{-2}\ s^{-1}$)			% of max light			Time before sunrise (min)			Light level ($\mu E\ m^{-2}\ s^{-1}$)			% of min light		
	mean	sd	*n*	**mean**	sd	*n*	**mean**	sd	*n*	**mean**	sd	*n*	**mean**	Sd	*n*	**mean**	sd	*n*
Jun 2011	**52**	41	12	**1074**	660	12	**43**	28	12	**49**	14	11	**5.8**	0.4	11	**167**	22	11
Jun 2010	**45**	55	7	**1016**	883	7	**41**	36	7	**56**	11	5	**4.6**	1.5	5	**243**	100	5
Nov 2008	**9**	24	7	–	–	–	–	–	–	**41**	0	1	–	–	–	–	–	–
Feb 2011	**13**	21	9	–	–	–	–	–	–	**41**	20	4	–	–	–	–	–	–
	End of ascent									End of descent								
	Time after sunset (min)			Light level ($\mu E\ m^{-2}\ s^{-1}$)			% of min light			Time after sunrise (min)			Light level ($\mu E\ m^{-2}\ s^{-1}$)			% of max light		
	mean	sd	*n*	**mean**	sd	*n*	**mean**	sd	*n*	**mean**	sd	*n*	**mean**	Sd	*n*	**mean**	sd	*n*
Jun 2011	**66**	19	12	**5.8**	0.6	12	**167**	19	12	**43**	28	11	**678**	529	11	**27**	21	11
Jun 2010	**49**	11	7	**5.5**	0.7	7	**294**	46	7	**15**	12	5	**234**	223	5	**9.2**	8.8	5
Nov 2008	**46**	17	7	–	–	–	–	–	–	**-1**	0	1	–	–	–	–	–	–
Feb 2011	**46**	20	9	–	–	–	–	–	–	**15**	23	4	–	–	–	–	–	–

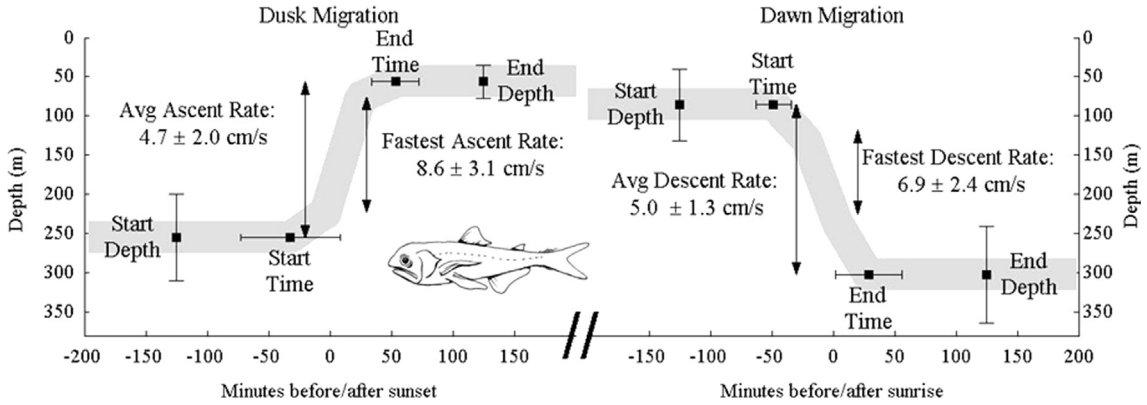

Fig. 5. Schematic of average rates and times of the diel vertical migration of the main scattering layer. Standard deviations are represented as error bars. Measured depths were of the bottom of the main migrating stratum. Grey background is a stylized layer and its width is not representative of true layer thickness. A cruise-by-cruise breakdown of times and average light levels are in Table 2, and migration rates are in Table 3.

Mean daytime depth of the background layer was 453 m, while a shallow upper stratum had a mean depth of 54 m and the mean daytime depth of the main migrating scattering layer was 332 m. In all cases except for the background layer depths in the Nov 2008 cruise, the day depths were significantly different than the nighttime depths. In aggregate, the background layer was 29 m deeper (95% confidence interval (CI) 18 to 40 m) during the day, the upper stratum was 18.5 m deeper (95% CI 13 to 24 m) at night, and the migrating layer was 278.5 m deeper (95% CI 270 to 287 m) during the day. Some statistically significant seasonal differences could be detected by comparing (using *t*-tests) the two June cruises with aggregated data from the Feb and Nov cruises. The daytime background layer in the June cruises was 128.5 m deeper (95% CI 104 to 153 m), the nighttime background layer was 110.5 m deeper (95% CI 84 to 137 m), the nighttime upper stratum was 13.5 m shallower (95% CI 6 to 21 m), and the daytime migrating stratum was 44.5 m deeper (95% CI 22 to 67 m) than during the Nov and Feb cruises.

The light levels and average time of migration initiation in relation to sunset/sunrise are displayed in Table 2. Aggregating data from both June cruises (the only ones with light data available), DVM of the main migrating scattering layer started on average 50 min before sunset, finished 60 min after sunset, started descending 51 min before sunrise and stabilized at depth 31 min after sunrise (Fig. 5). Organisms initiated migration when surface light levels were 1055 $\mu E\ m^{-2}\ s^{-1}$ on average (42% of maximum daytime light levels), but had finished their descent by the time surface light was 539 $\mu E\ m^{-2}\ s^{-1}$ (22% of maximum). There was no significant difference ($p=0.30$) between the light levels when migrators stopped ascending (5.7 $\mu E\ m^{-2}\ s^{-1}$) and started descending (5.4 $\mu E\ m^{-2}\ s^{-1}$). Descent in 2011 began with 1.2 $\mu E\ m^{-2}\ s^{-1}$ more light (95% CI 0.2 to 2.1) than in 2010, but 2011 also had a higher minimum light level due to a fuller moon.

DVM rates for the individual cruises are displayed in Table 3. Mean ascent rates ranged from 1.7 to 3.5 cm s^{-1} and max ascent rates ranged from 3.5 to 15.7 cm s^{-1}. DVM mean descent rates ranged from 2.0 to 7.4 cm s^{-1} and the max descent rates ranged from 2.0 to 13.3 cm s^{-1}. The average ascent rates over the fastest 100 m data were 1.7 cm s^{-1} (95% CI 0.2 to 3.3 cm s^{-1}) faster than the fastest descent rates. The ascent rates on the June cruises were 1.5 cm s^{-1} (95% CI 0.5 to 2.8 cm s^{-1}) slower than the ascent rates in Nov and Feb. The fastest ascent rates in June were 2.5 cm s^{-1} (95% CI 0.5 to 4.5 cm s^{-1}) slower than the fastest ascent rates in Nov and Feb. Other comparisons were not statistically significant.

3.2. Association with environmental parameters

Qualitatively, the most visually apparent association of scattering layers with environmental parameters was observed between the thermocline depth (which coincided generally with the pycnocline, halocline and oxycline) and the uppermost scattering layers. If the water column contained multiple background layers, most often the break came at the depth of the thermocline (e.g. Fig. 6A). The thermocline depth at each of the 103 CTD locations in the four study

areas was correlated ($R^2=0.60$) with the depth of the bottom of all scattering layers shallower than 120% of the thermocline depth. If only the deepest scattering layer bottom in this range was considered, the correlation was even stronger ($R^2=0.83$) and had a slope of 1.06 (Fig. 7). The strong correlation and the slope near one implied that this was a consistent phenomenon, and results of the tests below did not indicate any other explanations.

For layers deeper than the thermocline, it is clear why low-oxygen has been postulated to limit the depth of scattering layer organisms. Our results confirm the results of Dunlap (1968) and others that scattering layers generally are collocated in regions of low-oxygen. We continually found strong correlations between scattering layer depths and the depth of low-oxygen water. In the June 2011 data, for example, the depth of the 0.52 kPa isoline of oxygen was strongly correlated with the depth of the bottom of the 70 kHz background layer ($R^2=0.92$, slope=0.63, Fig. 8). Additionally, the edges of the background layer boundaries were much more distinct when the layers were associated with extreme values. Background layer boundaries were distinct when oxygen values were low (Fig. 6A and C), but were more diffuse when oxygen values did not drop to critical levels (Fig. 6B).

Other explanations for scattering layer depth could not be ruled out, however, from this initial test, as the correlations of the same layers with temperature ($R^2=0.6$) and density ($R^2=0.49$) were also strong, but with slopes much closer to one (1.02 and 1.07, respectively, Fig. 6). Additionally, when data from all four cruises were combined, these relationships were all much weaker. This result was not surprising, as many environmental parameters were tightly correlated (Table 4).

The second and third statistical tests confirmed that oxygen was not more influential statistically on scattering layer depth than other parameters. Of the >4000 χ^2 tests performed on different subsets of data (i.e. the subsets described in Section 2.4), in no more than 88 did oxygen have a significant ($p<0.05$) association with scattering layers when other parameters did not (Table 5). Similarly, even when the level of significance was increased to $p<0.10$), in no more than 82 tests was oxygen one of less than 3 parameters that were significant when depth was not.

The results of the logistic modeling pointed to temperature and density as more influential on scattering layer depths than oxygen. For data from all regions in water below the thermocline in the June 2011 cruise, in 1302 of 1598 models for the 38 kHz data and in 1292 of 1650 models for the 70 kHz data, temperature had the highest SOR (geometric means=403 and 9154, respectively, Table 6). Consistent with this interpretation, leaving temperature out of the June 2011, 38 kHz background layer bottom model increased the AIC from 1805 to 2090 and leaving density out of the model increased AIC to 2113, while at the same time reducing all

Table 3
DVM ascent and descent rates in the Gulf of California. Fastest rate is the rate measured over the most rapid rise/fall of 100 m.

	Ascent rate (cm s^{-1})						Descent rate (cm s^{-1})					
	Overall			Fastest			Overall			Fastest		
	mean	sd	*n*	**mean**	sd	*n*	**mean**	sd	*n*	**mean**	sd	*n*
Jun 2011	**3.3**	1.4	12	**7.2**	2.2	12	**4.5**	1.4	11	**7.0**	3.2	11
Jun 2010	**5.0**	2.3	7	**7.8**	2.9	7	**5.5**	0.7	5	**7.2**	1.2	5
Nov 2008	**6.0**	2.4	7	**10.2**	3.7	7	**6.0**	0.0	1	**6.0**	0.0	1
Feb 2011	**5.3**	1.4	9	**9.8**	3.3	9	**5.0**	1.3	4	**6.5**	1.7	4

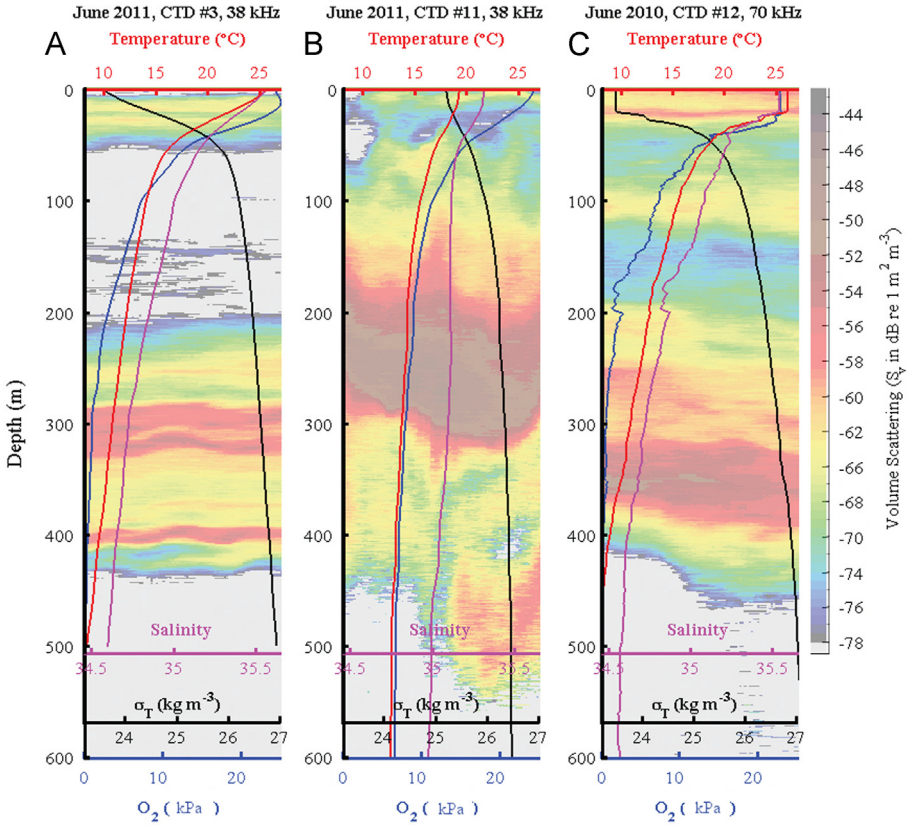

Fig. 6. Typical CTD profiles of temperature (T), oxygen (O_2), salinity (S), and potential density (σ_T), overlaying the acoustic scattering in the region the profile was collected. (A) A typical profile from the June 2011 cruise that includes severely hypoxic water above 600 m. (B) A typical CTD profile from the June 2011 cruise overlying scattering in a region that did not include severely hypoxic water. (C) From the June 2010 cruise. O_2 ranges from 23.2 kPa near the surface to 9.2 kPa at the thermocline to 2.0 kPa at 200 m. The range from 0 to 200 m is an order of magnitude larger than the range from 200 to 600 m.

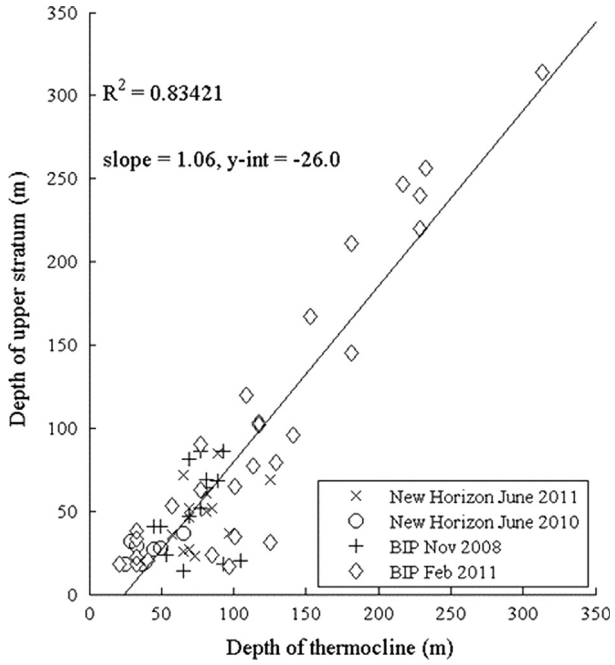

Fig. 7. Association between the depth of the thermocline and the bottom of the shallowest stratum in all 103 CTD regions. Displayed are the depths of the deepest scattering layer shallower than 120% of the depth of the thermocline in each CTD region.

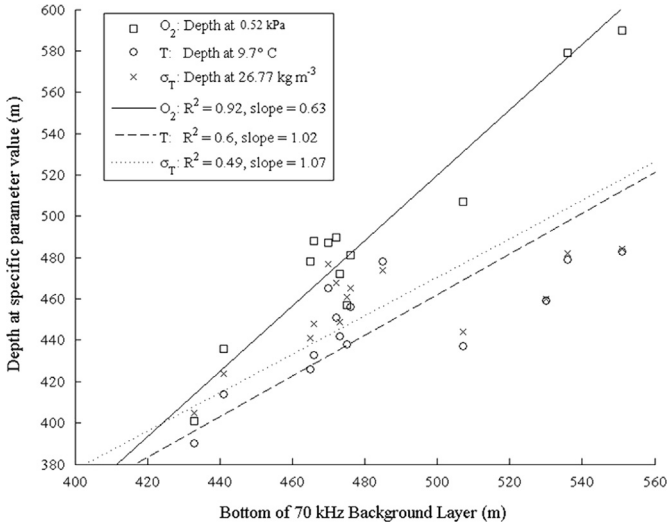

Fig. 8. Example correlations between the depth of the bottom of the background layer detected at 70 kHz and the depth of specific levels of oxygen, temperature, and density.

Table 4
Correlation coefficients (R^2) for measured parameters on the June 2011 research cruise.

T	Dens	S	O_2	PAR	dT	dDens	dS	dO_2	dPAR	
0.74	0.61	0.74	0.65	0.05	0.27	0.29	0.20	0.25	0.02	**Depth**
	0.96	0.90	0.94	0.16	0.47	0.53	0.31	0.32	0.07	**T**
		0.76	0.89	0.22	0.54	0.61	0.34	0.32	0.09	**Dens**
			0.91	0.11	0.32	0.36	0.23	0.25	0.05	**S**
				0.16	0.50	0.55	0.34	0.36	0.07	**O_2**
					0.06	0.08	0.04	0.01	0.52	**PAR**
						0.98	0.81	0.75	0.03	**dT**
							0.72	0.68	0.03	**dDens**
								0.78	0.01	**dS**
									0.01	**dO_2**

SORs to less than 1.55, implying that temperature and density are both critical variables in the model. Additionally, leaving either temperature or density out of the model severely limited the ability of the model to accurately predict features (graph I in Fig. 4). Leaving salinity out, in contrast, only increased AIC to 1822 and leaving oxygen out increased AIC to 1868. Neither removal, nor the removal of any of the gradients of any parameters, greatly affected the model and so those results were not included in Fig. 4.

There was some evidence that light was influential on the depth of daytime mid-water (thermocline-400 m) scattering layers. While leaving light out of the logistic models had very little effect on deeper features, graphs III–V in Fig. 4 highlight the negative effects on the models when light is removed, although in all these cases temperature still had the highest SOR. Additionally, in the 114 tests in the June 2011 70 kHz data where light was one of <3 significant factors and depth was non-significant, all but one were with mid-water scattering layers.

4. Discussion

In all seasons considered in this research, scattering layers were consistently found in most regions of the central Gulf of California at all times of day at a variety of depths down to 600 m. Although Jaquet and Gendron (2002) anecdotally reported only weak scattering layers in the summer in the Gulf of California, our analysis confirmed results of others (Fiedler et al., 1998; Gilly et al., 2006; Markaida et al., 2008) that acoustic scattering layers are an obvious and likely significant component of the ecosystem in this region throughout the year. In general, background scattering layers were broad, up to several hundred meters in width but had inconsistent internal structure. Discretely definable acoustic structures within these layers tended to be more consistent (Fig. 2). These internal strata were typically <100 m in width, but contained the bulk of the acoustic energy in the water column.

During daylight hours we observed consistent scattering layer bottom boundaries at 45 and 325 m, with the boundary of the background scattering layer occurring between 340 and 485 m. These observations were consistent with Dunlap's (1968) results from a broader region in the Gulf of California that includes our study region. Daytime scattering layers in this region in Sep–Nov were around 175, 300, 400 and sometimes 500 m depth. The largest difference between then and now was Dunlap's report that the most common 30 kHz scattering layer was between 100 and 200 m, between the 13 and 14° isotherms, while in our survey, this depth zone commonly contained 38 kHz scattering layers only during dusk and dawn migration events. This region did often contain a higher frequency (120 kHz) layer, however, suggesting some size differentiation or potentially a change in species over the last 50 years. It is also possible that the two surveys actually detected the same layer, but differences in bandwidth in our equipment resulted in differentiation of this layer as strictly high-frequency in our surveys. Consistent with our results, Dunlap reported that the deepest scattering layer in the Gulf of California was associated with low oxygen levels (<0.2 mL L^{-1}), similar to our observation that the bottom of the background layer in June 2011 was correlated with oxygen levels of 0.15 mL L^{-1} (0.52 kPa).

Diel vertical migrations of the deep scattering layer within the survey area were typical "nocturnal migrations" (Cohen and Forward, 2009) comprised of a single twilight ascent (average 4.7 cm s^{-1}, maximum 8.6 cm s^{-1}) and dawn descent (average 5.0 cm s^{-1}, maximum 6.9 cm s^{-1}). Movement rates were comparable to those found for scattering layers in the similarly subtropical Gulf of Mexico (Kaltenberg et al., 2007). As with the migration timing, the light levels during migration were similar to those reported for the area 50 years ago with surface light levels in our study at ascent initiation of

Table 5
Results of the second statistical method, χ^2 analyses for non-random patterns in the association of environmental parameters with scattering layer features. d___ is short-hand for d__/dz, the gradient of each parameter with respect to depth. (A) The number of time that each tested parameter was one of three or fewer parameters with $p < 0.1$ when depth did not show a non-random association with the scattering layer feature ($p > 0.05$). (B) The number of occurrences where the parameter is the only significant ($p < 0.05$) association.

A.

Cruise	Freq	Temp	O_2	Dens	Salin	Light	dTemp	dO_2	dDens	dSalin	dLight
June 2011	38 kHz	69	67	42	39	34	11	64	14	29	70
June 2011	70 kHz	59	82	30	63	114	8	5	22	15	59
Both June	38 kHz	50	54	50	54	–	13	52	6	30	–
Both June	70 kHz	86	22	75	32	–	4	1	22	9	–
All	38 kHz	3	11	8	8	–	–	–	–	–	–

B.

Cruise	Freq	Temp	O_2	Dens	Salin	Light	dTemp	dO_2	dDens	dSalin	dLight
June 2011	38 kHz	42	88	11	30	18	8	65	10	20	60
June 2011	70 kHz	18	60	5	27	87	0	3	20	8	49
Both June	38 kHz	15	34	17	27	–	10	45	0	8	–
Both June	70 kHz	7	22	17	33	–	2	2	21	8	–
All	38 kHz	1	7	11	3	–	–	–	–	–	–

Table 6
Geometric means of the standardized odds ratio (SOR) of the coefficients of logistic models predicting the depth of scattering layer features. Layer features examined in this subset were the entire layer, the layer bottom, and the peak energy of the layer. Displayed values are means from models built using all geographic regions, from layers occurring below the thermocline. The coefficients of 1598 models were averaged for the 38 kHz data, and 1650 models for the 70 kHz data. d___ is short-hand for d__/dz, the gradient of each parameter with respect to depth.

Cruise	Freq	Depth	Temp	O_2	Dens	Salin	Light	Fluor	dTemp	dO_2	dDens	dSalin	dLight	dFluor
June 2011	38 kHz	1.3	403	3	80	17	1.1	1.0	1.7	1.1	1.5	1.4	1.0	1.0
June 2011	70 kHz	2.7	9154	17	717	88	1.1	1.4	665	7.7	51	11	1.5	1.0

$42 \pm 31\%$ of the maximum of that day, whereas Dunlap (1968) reported a similar value (within one standard error) of 66% during a single observation. Although Dunlap's study was less specific than ours, the lack of significant differences between our results and Dunlap's suggest that both scattering layer organisms, which serve as fundamental links between phytoplankton and larger predators, and the conditions which cue these animals are not discernibly different than they were 50 years ago, despite large changes in the Gulf in general. Stewart et al. (2014) found evidence supporting the correlation between myctophid and hake abundance and Humboldt squid abundance in Monterey Bay, California. Our results, however, present an interesting puzzle in that the dominant predators in the region seem to have shifted from tuna and billfish to Humboldt squid (Sagarin et al., 2008) despite a lack of obvious changes in acoustic scattering layers, a proxy for the ecology of lower trophic levels.

It has been proposed that changes in the oxygen minimum zone depth could be affecting the depth and density of scattering layers and that these conditions could be favorable for Humboldt squid (Gilly et al., 2013; Stewart et al., 2013). In support of this hypothesis, prior research (e.g. Robison, 1972; Bertrand et al., 2010; Bianchi et al., 2013) has found correlations between specific oxygen values and scattering layers, and inferred that the low oxygen in deep waters has a limiting effect on the depth of the organisms found in the layers. However, while Bianchi et al. (2013) found a general, less localized pattern of DVM depths coinciding with the upper-margins of low-oxygen waters, similar to our results they found that models including multiple variables were better descriptors of scattering layer depths than models relying just on a single parameter. Our results are more in alignment with Childress and Seibel's (1998) hypothesis: not only is separating the influence of different parameters difficult, but many of the organisms that comprise scattering layers are particularly well adapted to these environments, so it is likely that other parameters have larger influences than oxygen on scattering layer depth. It is also possible, as proposed by Bianchi et al. (2013), that it is the respiration of these abundant creatures at depth that contributes to the low oxygen at their daytime depths, indicating that it may not be low oxygen waters that cause migrators to stop their descent, but the other way around.

Despite multiple methods of analysis of our data, no environmental parameter universally indicated scattering layer presence. Our preliminary hypothesis was that oxygen would be a strong controlling factor of layer depth as suggested by other studies (i.e. Bertrand et al., 2010). In contrast, our results do not support the O_2-limited hypothesis, despite the presence of correlations between the bottom of the background layer and isolines of oxygen. Further analysis gave evidence that light levels were associated with scattering layer depths in mid-water (below the thermocline) regions, and that temperature and/or density were more associated with scattering layer depths than any other parameter which may help explain some of the changes in *Dosidicus* distribution during ENSO events (Rosas-Luis et al., 2008; Hoving et al., 2013). Oxygen's contribution to the success of the logistic models was not substantial in the vast majority of the models that were run, indicating that, despite correlations, oxygen levels were not predictive of scattering layer depths.

In support of alternative explanations, Wang et al. (2014) found that in the Persian Gulf light is a dominant influence on scattering layer features and that temperature and salinity are as much or of more importance than oxygen. In our dataset, Fig. 9 shows several associations of scattering layers with bends in plots of temperature vs. salinity, implying that at least some features (in addition to the shallow features associated with the thermocline) are associated with boundaries between water masses. Childress and Seibel (1998) offer an explanation for these associations: myctophids and other scattering layer organisms can conserve energy by spending non-feeding time in cooler, deeper water, and thus oxygen content may only be of secondary importance.

Scattering layer organisms contend with a range of competing environmental and social cues, and it is clear that simple correlations

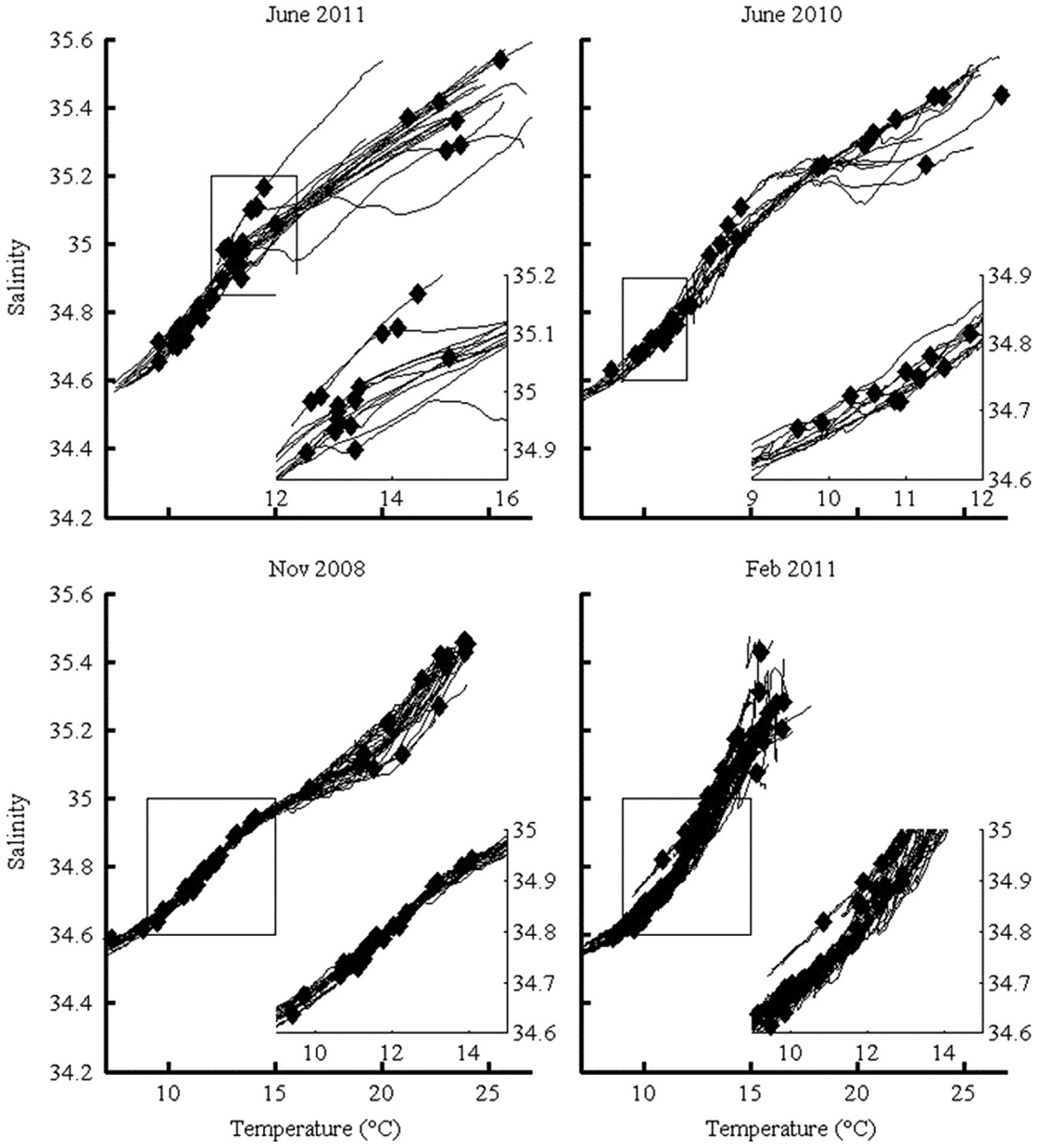

Fig. 9. Temperature-salinity plots of every CTD profiles from the four cruises. Black diamonds are the temperature and salinity at the depths of the peak energy of all detected core strata in each region. The regions in the boxes are expanded in the insets. While some strata appear at sharp changes in the profile, implying that they could be associated with water mass changes, it is not a consistent explanation.

of scattering layer depths to environmental parameters are insufficient for disentangling the influences of oceanographic parameters that are highly correlated. Covariance among environmental parameters is often a facet of oceanographic studies, and, when inferring causation from correlations between organisms and their habitat, covariance must be considered not just statistically, from the standpoint of independence of variables, but from a biological and oceanographic context. Ideally, this problem of covarying parameters could be more thoroughly examined with a long-term analysis at a single location where oceanographic parameters vary enough to provide a decoupling of parameter values over time (as also suggested by Childress and Seibel, 1998), but this scenario is much more common in shallow, coastal waters (e.g. Adams et al., 2013) than in deep pelagic environments. If such a scenario could be studied, the analytical techniques we have described could more effectively isolate an indicator parameter. While there is evidence from our study that shallow scattering layers are associated with environmental gradients (i.e. the thermocline), and mid-water scattering layers show some important associations with light levels, the deeper scattering layers do not show a strong association with low-oxygen levels as was predicted, and care should be taken in future studies to report other possible environmental explanations for the vertical distributions of these important organisms.

In the Gulf of California, our results are in agreement with others that the deepest daytime scattering layer at ~400 to 600 m usually occurs in a hypoxic area (Robison, 1972). However, our results also concur with Dunlap (1968) who found that scattering layers do not appear to have a specific association with oxyclines or specific oxygen values, but that temperature may serve as an indicator of layer depth. While a shoaling OMZ certainly has implications for many species, many denizens of deep scattering layers are well-adapted to low-oxygen conditions (Seibel, 2011), and it does not appear that a shoaling OMZ greatly reduces the habitat of scattering layer organisms as has been proposed (Gilly

et al., 2013). If predators like the Humboldt squid are benefitting from a shoaling OMZ, it is likely not from habitat compression of prey in deep scattering layers, but could instead be either from changes in behavior resulting from exposure to low-oxygen waters or from the overlap of the habitats of predator and prey that results when the low-oxygen water to which squid are well-adapted is brought closer to the scattering layer organisms on which they feed, potentially reducing competition between squid and other scattering layer predators.

In the Gulf of California, mid-water zooplankton and nekton form consistent and extensive scattering layers with clearly definable boundaries that migrate in unison: upwards at night and downwards during the day. Despite dramatic changes in the Gulf of California over the last fifty years, the overall depths and diel patterns of these midwater features are relatively consistent with an earlier survey. The concentrations of single environment parameters, including oxygen, were shown to not be solely indicative of scattering layer depths, implying that many factors are influencing the behavior of scattering layer organisms. Thus, changes in the scattering layers in the Gulf of California or the relationships between these mesopelagic animals and the environment are unlikely to be the primary factor accountable for the dramatic changes observed in the system, including the recent success of *D. gigas*. These abundant, ubiquitous, and robust aggregations may represent a predictable and stable resource to many predators in the face of a rapidly changing environment.

Acknowledgements

The authors wish to thank Emily Shroyer and Scott Heppell for manuscript feedback, and Chad Waluk for technical assistance. We also wish to thank the US Office of Naval Research (N00014-11-1-0146) for dedicated support of the data analysis and the National Science Foundation (0851239) for support of data collection efforts.

References

Adams, K.A., Barth, J.A., Chan, F., 2013. Temporal variability of near-bottom dissolved oxygen during upwelling off central Oregon. J. Geophys. Res. Oceans 118 (10), 4839–4854.
Barham, E.G., 1966. Deep scattering layer migration and composition: observations from a diving saucer. Science 151 (3716), 1399–1403.
Benoit-Bird, K.J., Au, W.W.L., 2002. Energy: converting from acoustic to biological resource units. J. Acoust. Soc. Am. 111 (5), 2070–2075.
Benoit-Bird, K.J., Gilly, W.F., 2012. Coordinated nocturnal behavior of foraging jumbo squid *Dosidicus gigas*. Mar. Ecol. Prog. Ser. 455, 211–228.
Bertrand, A., Ballón, M., Chaigneau, A., 2010. Acoustic observation of living organisms reveals the upper limit of the oxygen minimum zone. PLoS One 5 (4), e10330.
Bianchi, D., Galbraith, E.D., Carozza, D.A., Mislan, K., Stock, C.A., 2013. Intensification of open-ocean oxygen depletion by vertically migrating animals. Nat. Geosci. 6 (7), 545–548.
Burd, B.J., Thomson, R.E., Jamieson, G.S., 1992. Composition of a deep scattering layer overlying a mid-ocean ridge hydrothermal plume. Mar. Biol. 113 (3), 517–526.
Butler, J.L., Pearcy, W.G., 1972. Swimbladder morphology and specific gravity of myctophids off Oregon. J. Fish. Board Can. 29 (8), 1145–1150.
Cade, D.E., Benoit-Bird, K.J., 2014. An automatic and quantitative approach to the detection and tracking of acoustic scattering layers. Limnol. Oceanogr. Methods 12, 742–756.
CEC, 2009. Baja to Bering Region. Commission for Environmental Cooperation, Montréal, Québec, Canada.
Chapman, R., Marshall, J., 1966. Reverberation from deep scattering layers in the western North Atlantic. J. Acoust. Soc. Am. 40 (2), 405–411.
Childress, J.J., Seibel, B.A., 1998. Life at stable low oxygen levels: adaptations of animals to oceanic oxygen minimum layers. J. Exp. Biol. 201 (8), 1223–1232.
Clarke, G.L., 1970. Light conditions in the sea in relation to the diurnal vertical migrations of animals. In: Proceedings of an International Symposium on Biological Sound Scattering in the Ocean. Department of the Navy, Washington, DC, pp. 41-50.
Cohen, J.H., Forward, R.B., Jr, 2009. Zooplankton diel vertical migration—a review of proximate control. In: Gibson, R., Atkinson, R., Gordon, J. (Eds.), Oceanography and Marine Biology: An Annual Review. CRC Press, Boca Raton, pp. 77-110.
Cohen, J.H., Forward Jr., R.B., 2005. Diel vertical migration of the marine copepod *Calanopia americana* I. Twilight DVM and its relationship to the diel light cycle. Mar. Biol. 147 (2), 387–398.
Devol, A.H., 1981. Vertical distribution of zooplankton respiration in relation to the intense oxygen minimum zones in two British Columbia fjords. J. Plankton Res. 3 (4), 593–602.
Dunlap, C.R., 1968. An Ecological Reconnaissance of the Deep Scattering Layers in the Eastern Tropical Pacific, Monterey, California. Naval Postgraduate School, Monterey, CA.
Fiedler, P.C., Barlow, J., Gerrodette, T., 1998. Dolphin prey abundance determined from acoustic backscatter data in eastern Pacific surveys. Fish. Bull. 96 (2), 237–247.
Fock, H.O., Matthiessen, B., Zidowitz, H., Westernhagen, H.v., 2002. Diel and habitat-dependent resource utilisation by deep-sea fishes at the Great Meteor seamount: niche overlap and support for the sound scattering layer interception hypothesis. Mar. Ecol. Prog. Ser. 244, 219–233.
Forward Jr., R.B., 1976. Light and diurnal vertical migration: photobehavior and photophysiology of plankton. In: Smith, K.C. (Ed.), Photochemical and Photobiological Reviews. Plenum Press, New York, pp. 157–210.
Forward Jr., R.B., Wellins, C.A., 1989. Behavioral responses of a larval crustacean to hydrostatic pressure: *Rhithropanopeus harrisii* (Brachyura: Xanthidae). Mar. Biol. 101 (2), 159–172.
Gilly, W., Markaida, U., Baxter, C., Block, B., Boustany, A., Zeidberg, L., Reisenbichler, K., Robison, B., Bazzino, G., Salinas, C., 2006. Vertical and horizontal migrations by the jumbo squid *Dosidicus gigas* revealed by electronic tagging. Mar. Ecol. Prog. Ser. 324, 1–17.
Gilly, W.F., Beman, J.M., Litvin, S.Y., Robison, B.H., 2013. Oceanographic and biological effects of shoaling of the oxygen minimum zone. Annu. Rev. Mar. Sci. 5, 393–420.
Hays, G.C., 2003. A review of the adaptive significance and ecosystem consequences of zooplankton diel vertical migrations. Hydrobiologica 503, 163–170.
Herdman, H., 1953. The deep scattering layer in the sea: association with density layering. Nature 172, 275–276.
Hofmann, A., Peltzer, E., Walz, P., Brewer, P., 2011. Hypoxia by degrees: establishing definitions for a changing ocean. Deep Sea Res. Part I Papers 58 (12), 1212–1226.
Hoving, H.J.T., Gilly, W.F., Markaida, U., Benoit-Bird, K.J., Brown, Z.W., Daniel, P., Field, J.C., Parassenti, L., Liu, B., Campos, B., 2013. Extreme plasticity in life-history strategy allows a migratory predator (jumbo squid) to cope with a changing climate. Global Change Biol. 19 (7), 2089–2103.
Instituto Nacional de Estadística y Geografía, 2014. Statistics. ⟨http://www3.inegi.org.mx/sistemas/mexicocifras/⟩.
Irigoien, X., Klevjer, T., Røstad, A., Martinez, U., Boyra, G., Acuña, J., Bode, A., Echevarria, F., Gonzalez-Gordillo, J., Hernandez-Leon, S., 2014. Large mesopelagic fishes biomass and trophic efficiency in the open ocean. Nat. Commun. 5.
Jaquet, N., Gendron, D., 2002. Distribution and relative abundance of sperm whales in relation to key environmental features, squid landings and the distribution of other cetacean species in the Gulf of California, Mexico. Mar. Biol. 141 (3), 591–601.
Kaltenberg, A.M., Biggs, D.C., DiMarco, S.F., 2007. Deep scattering layers of the northern Gulf of Mexico observed with a ship-board 38-kHz acoustic Doppler current Profiler (ADCP). Gulf of Mexico Sci. 2, 97–108.
Kumar, P.V.H., Kumar, T.P., Sunil, T., Gopakumar, M., 2005. Observations on the relationship between scattering layer and mixed layer. Curr. Sci. 88 (11), 1799.
Kunze, E., Dower, J.F., Beveridge, I., Dewey, R., Bartlett, K.P., 2006. Observations of biologically generated turbulence in a coastal inlet. Science 313 (5794), 1768–1770.
Longhurst, A., Bedo, A., Harrison, W., Head, E., Sameoto, D., 1990. Vertical flux of respiratory carbon by oceanic diel migrant biota. Deep Sea Res. Part A Papers 37 (4), 685–694.
Markaida, U., Gilly, W.F., Salinas-Zavala, C.A., Rosas-Luis, R., Booth, J., 2008. Food and Feeding of Jumbo Squid *Dosidicus gigas* in the Central Gulf of California during 2005-2007. California Cooperative Oceanic Fisheries Investigations Report 49, 90-103.
McGehee, D., O'Driscoll, R., Traykovski, L.M., 1998. Effects of orientation on acoustic scattering from Antarctic krill at 120 kHz. Deep-Sea Res. Part II 45 (7), 1273–1294.
O'Brien, D.P., 1987. Direct observations of the behavior of *Euphausia superba* and *Euphausia crystallorophias* (Crustacea: Euphausiacea) under pack ice during the Antarctic spring of 1985. J. Crustacean Biol. 7 (3), 437–448.
Opdal, A., Godø, O., Bergstad, O., Fiksen, Ø., 2008. Distribution, identity, and possible processes sustaining meso-and bathypelagic scattering layers on the northern Mid-Atlantic Ridge. Deep Sea Res. Part II 55 (1), 45–58.
Ramsey, F.L., Schafer, D.W., 2013. The Statistical Sleuth: A Course in Methods of Data Analysis. Brooks/Cole, United States of America.
Robison, B.H., 1972. Distribution of the midwater fishes of the Gulf of California. Copeia 1972 (3), 448–461.
Robles, J.M., Marinone, S., 1987. Seasonal and interannual thermohaline variability in the Guaymas Basin of the Gulf of California. Cont. Shelf Res. 7 (7), 715–733.
Rodriguez, C.A., Flessa, K.W., Dettman, D.L., 2001. Effects of upstream diversion of Colorado River water on the estuarine bivalve mollusc *Mulinia coloradoensis*. Conserv. Biol. 15 (1), 249–258.
Rosa, R., Seibel, B.A., 2010. Metabolic physiology of the Humboldt squid, *Dosidicus gigas*: implications for vertical migration in a pronounced oxygen minimum zone. Prog. Oceanogr. 86 (1), 72–80.

Rosas-Luis, R., Salinas-Zavala, C., Koch, V., Luna, P., Morales-Zárate, M., 2008. Importance of jumbo squid *Dosidicus gigas* (Orbigny, 1835) in the pelagic ecosystem of the central Gulf of California. Ecol. Modell. 218 (1), 149–161.

Rusnak, G.A., Fisher, R.L., Shepard, F.P., 1964. Bathymetry and faults of Gulf of California. In: van Andel, T.H., Shor Jr., G.G. (Eds.), Marine Geology of the Gulf of California. American Association of Petroleum Geologists, Tulsa, OK, pp. 59–75.

Sagarin, R.D., Gilly, W.F., Baxter, C.H., Burnett, N., Christensen, J., 2008. Remembering the Gulf: changes to the marine communities of the Sea of Cortez since the Steinbeck and Ricketts expedition of 1940. Front. Ecol. Environ. 6 (7), 372–379.

Sameoto, D., 1976. Distribution of sound scattering layers caused by euphausiids and their relationship to chlorophyll *a* concentrations in the Gulf of St. Lawrence Estuary. J. Fish. Board of Can. 33 (4), 681–687.

Seibel, B.A., 2011. Critical oxygen levels and metabolic suppression in oceanic oxygen minimum zones. J. Exp. Biol. 214 (2), 326–336.

Simard, Y., Mackas, D.L., 1989. Mesoscale aggregations of euphausiid sound scattering layers on the continental shelf of Vancouver Island. Can. J. Fish. Aquat. Sci. 46 (7), 1238–1249.

Steinbeck, J., Ricketts, E.F., 1941. Sea of Cortez; A Leisurely Journal of Travel and Research, with a Scientific Appendix Comprising Materials for a Source Book on the Marine Animals of the Panamic Faunal Province. PP Appel, Mamaroneck, NY.

Steinberg, D.K., Carlson, C.A., Bates, N.R., Goldthwait, S.A., Madin, L.P., Michaels, A.F., 2000. Zooplankton vertical migration and the active transport of dissolved organic and inorganic carbon in the Sargasso Sea. Deep Sea Res. Part I Papers 47 (1), 137–158.

Stewart, J.S., Field, J.C., Markaida, U., Gilly, W.F., 2013. Behavioral ecology of jumbo squid (*Dosidicus gigas*) in relation to oxygen minimum zones. Deep Sea Res. Part II 95, 197–208.

Stewart, J.S., Hazen, E.L., Bograd, S.J., Byrnes, J.E., Foley, D.G., Gilly, W.F., Robison, B. H., Field, J.C., 2014. Combined climate-and prey-mediated range expansion of Humboldt squid (*Dosidicus gigas*), a large marine predator in the California Current System. Global Change Biol. 20 (6), 1832–1843.

Thomson, R.E., Burd, B.J., Dolling, A.G., Lee Gordon, R., Jamieson, G.S., 1992. The deep scattering layer associated with the Endeavour Ridge hydrothermal plume. Deep Sea Res. Part A Papers 39 (1), 55–73.

Tont, S.A., 1976. Deep Scattering Layers: Patterns in the Pacific. California Cooperative Oceanic Fisheries Investigations Report 18, 112-117.

Wackerly, D.D., Mendenhall, W., Scheaffer, R.L., 2008. Mathematical Statistics with Applications. Thomson Brooks/Cole, Belmont, CA.

Wang, Z., DiMarco, S.F., Ingle, S., Belabbassi, L., Al-Kharusi, L.H., 2014. Seasonal and annual variability of vertically migrating scattering layers in the northern Arabian Sea. Deep Sea Res. Part I Papers 90, 152–165.

Weston, D., 1958. Observations on a scattering layer at the thermocline. Deep-Sea Res. 5 (1), 44–50.